Magnetic self-field effects on current collection by an ionospheric bare tether

J. R. Sanmartín
Escuela Tecnica Superior de Ingenieros Aeronáuticos, Universidad Politécnica de Madrid, Madrid, Spain

R. D. Estes
Harvard-Smithsonian Center for Astrophysics, Cambridge, Massachusetts, USA

Received 22 February 2002; revised 12 July 2002; accepted 21 August 2002; published 2 November 2002.

[1] It was recently suggested that the magnetic field created by the current of a bare tether strongly reduces its own electron-collection capability when a magnetic separatrix disconnecting ambient magnetized plasma from tether extends beyond its electric sheath. It is here shown that current reduction by the self-field depends on the ratio L_*/L_t parameterizing bias and current profiles along the tether ($L_t \equiv$ tether length, $L_* \equiv$ characteristic length gauging ohmic effects) and on a new dimensionless number K_s involving ambient and tether parameters. Current reduction is weaker the lower K_s and L_*/L_t, which depend critically on the type of cross section: K_s varies as $R^{5/3}$, $h^{2/3}R$, and $h^{2/3} \times 1/4$ width for wires, round tethers conductive only in a thin layer, and thin tapes, respectively; L_* varies as $R^{2/3}$ for wires and as $h^{2/3}$ for tapes and round tethers conductive in a layer ($R \equiv$ radius, $h \equiv$ thickness). Self-field effects are fully negligible for the last two types of cross sections whatever the mode of operation. In practical efficient tether systems having L_*/L_t low, maximum current reduction in case of wires is again negligible for power generation; for deorbiting, reduction is <1% for a 10 km tether and ~15% for a 20 km tether. In the reboost mode there are no effects for K_s below some threshold; moderate effects may occur in practical but heavy reboost-wire systems that need no dedicated solar power. *INDEX TERMS:* 7807 Space Plasma Physics: Charged particle motion and acceleration; 7815 Space Plasma Physics: Electrostatic structures; 7853 Space Plasma Physics: Spacecraft/atmosphere interactions; 7855 Space Plasma Physics: Spacecraft sheaths, wakes, charging; *KEYWORDS:* ionospheric tethers, bare tethers, magnetic self-field of tethers, magnetic effects on current collection, orbital-motion-limited current, magnetic topology

Citation: Sanmartin, J. R., and R. D. Estes, Magnetic self-field effects on current collection by an ionospheric bare tether, *J. Geophys. Res.*, *107*(A11), 1335, doi:10.1029/2002JA009344, 2002.

1. Introduction

[2] The interaction of a conductive space tether with ionosphere and ambient magnetic field has potential applications that range from spacecraft reboost or deorbiting to onboard power generation and optimal generation of an electron beam. A basic issue with tethers is electron collection from the rarefied ionosphere. It was proposed that the tether itself, if left uninsulated, would efficiently collect electrons over its anodic segment [*Sanmartín et al.*, 1992, 1993]. A bare tether works as a cylindrical Langmuir probe; bias varies along its length but typical values of length-to-thickness ratio are of the order of 10^6, bare tethers thus collecting current per unit length at each point as if uniformly polarized at the local bias. A full analysis of electron collection by tether systems requires a detailed theory of highly positive, two-dimensional (2-D) probes with thickness comparable to the electron Debye length λ_D. That theory has been fairly advanced recently.

[3] It was long known that the current I to an electron-attracting cylinder has an upper bound I_{OML} that is independent of the cross section shape if convex: it does not require a rotationally symmetric potential [*Laframboise and Parker*, 1973]. At high bias, I_{OML} is proportional to square root of bias ΔV, in addition to being proportional to plasma density N_∞ and tether length L and cross section perimeter p,

$$\frac{I_{OML}(p)}{L} \approx \frac{p}{\pi} \times eN_\infty \times \sqrt{\frac{2e\Delta V}{m_e}}. \qquad (1)$$

For circular cross sections, this 2-D orbital motion limited (OML) bound is reached for radius R less than some maximum radius R_{max}, recently determined by way of an asymptotic analysis [*Sanmartín and Estes*, 1999]; for typical values $T_i \approx T_e$ and $e\Delta V \approx 10^2 - 10^4 kT_e$ one has $R_{max} \approx 0.9\lambda_D$. For $R > R_{max}$ the ratio $I/I_{OML}(p)$ is a function $G(R/\lambda_D, e\Delta V/kT_e, T_i/T_e)$, current I thus separately depending

0148-0227/02/2002JA009344

on both radius and perimeter [*Estes and Sanmartín*, 2000]. The above results hold for an arbitrary convex cross section if R is replaced in G by certain "equivalent" radius R_{eq}; for a thin tape of width w, one finds $R_{eq} = w/4 = p/8$. For nonconvex cross sections one must also replace p by some equivalent perimeter p_{eq} (e.g., $p_{eq}/6.55 \approx R_{eq} = \pi c/2$ for a cross section made of two adjoining circles of radius c). For cross sections made of disjoint parts, certain "effective" perimeter p_{eff} replaces p; tethers made of multiple parallel lines to enhance survivality will have disjoint cross sections [*Sanmartín and Estes*, 2001].

[4] All above results apply to unmagnetized plasmas at rest, with faraway electron population isotropic and with no electrons trapped in bound trajectories. Tethers, however, move through a plasma at relative speed U_{sat} in the presence of the geomagnetic field B_0. Bare tether collection will be tested in orbit in early 2003 by the NASA experiment Propulsive Small Expendable Deployer System [*Johnson et al.*, 2000]; preliminary results from laboratory tests and PIC calculations tentatively indicate that any U_{sat} or B_0 effects would not decrease the current collected. As regards U_{sat} effects, the I_{OML} bound might still hold because that mesothermal speed barely breaks electron isotropy. However, a well-known theorem on the density of collisionless electrons in 2-D potential wells [*Laframboise and Parker*, 1973] could imply that a substantial trapped-electron population is required to keep plasma quasi-neutral over large regions. Collisional trapping rates prove too slow to be of consequence [*Sanmartín and Estes*, 1999], but adiabatic collisionless trapping [*Gurevich*, 1968] might be [*Onishi et al.*, 2001].

[5] As regards B_0 the 2-D OML bound might not hold, in general, in a magnetized plasma because of 3-D considerations [*Laframboise and Rubinstein*, 1976]. There exists however another upper (Parker-Murphy) bound; at high bias that bound reads

$$I_{PM} \approx \sqrt{\frac{2}{\pi}} \times \frac{l_{e0}}{R} \times I_{OML}, \tag{2}$$

where $l_{e0} \equiv v_{th}/\Omega_0$ is gyroradius and $v_{th} \equiv \sqrt{kT_e/m_e}$ and Ω_0 are electron thermal velocity and gyrofrequency, respectively. Clearly, for $l_{e0} \gg R$ this upper bound is well above I_{OML}; the geomagnetic field might then be expected to hardly affect the current. Actually, the Parker-Murphy (PM) bound all but ignores space charge; it has been suggested that an additional condition ($l_{e0} \gg \lambda_D$) is required for B_0 effects to be negligible [*Sanmartín and Estes*, 1999]. Such effects could thus only apply for l_{e0} that is not too large.

[6] Here we consider a recent suggestion that the magnetic field B_s created by the tether current could be so large as to substantially reduce collection by a bare tether [*Khazanov et al.*, 2000, 2001] even if B_0 does not. This would be important because no such effects would affect current to tether-end devices. In section 2 we recall and discuss the condition suggested by Khazanov et al. as characterizing self-field effects. In section 3 we show that a simple conservative form of the condition relates a single dimensionless number involving ambient and tether parameters to the current-voltage profiles along the tether, both depending critically on the type of tether cross section. Effects for drag/power generation and thrust modes in efficient tether systems are discussed in sections 4 and 5, respectively. Results are resumed in section 6.

2. Magnetic-Separatrix Versus Electric-Sheath Condition

[7] *Khazanov et al.* [2000] showed that the self-field B_s from a circular wire modifies the topology of magnetic field lines in the cross-section plane: there now exists a closed separatrix, field lines being open outside it (as in the case of zero B_s) and closed inside, a Parker-Murphy analysis then leading to a reduction in the PM current bound. More important, they suggested a criterion to determine when the actual current is strongly reduced. The argument involves a characteristic dimension of the separatrix, taken as the distance r^* from tether axis that results from equating fields B_0 and $B_s = I/2\pi\varepsilon_0 c^2 r$ (in SI units),

$$r^* = I/2\pi\varepsilon_0 c^2 B_0. \tag{3}$$

Actually, the entire separatrix scales with the distance $r^*/\cos\alpha$ where $B_s = B_0 \cos\alpha$ (projection of $\overline{B}_0$ on the cross-section plane, at angle α). In polar coordinates r, ϕ in that plane the separatrix can be written as

$$\ln\left(\frac{r}{r^*/\cos\alpha}\right) + \frac{r}{r^*/\cos\alpha}\cos\phi + 1 = 0,$$

with $\phi = \pi/2$ along the $\overline{B}_0$ projection.

[8] The criterion for strong self-field effects requires the plasma sheath to lie inside the separatrix in some average sense. *Khazanov et al.* [2000] first assumed no electron collection under condition $r_{sh} + l_{ef} < ar^*$, with full collection otherwise; here a is some appropriate coefficient, and r_{sh} and l_{ef} ($\ll r_{sh}$) are sheath radius and a local gyroradius, which accounts for a small thermal flux accross the separatrix. They later refined the criterion by estimating how collection is reduced but not fully suppressed under the weaker condition

$$r_{sh} < ar^*, \tag{4}$$

with full collection otherwise [*Khazanov et al.*, 2001].

[9] We shall here use the condition in equation (4), assuming, however, no collection when equation (4) holds. This slight overestimate of B_s effects is conservative for the purpose of showing such effects to be weak, and it greatly simplifies the discussion. Self-field effects will appear greater the greater coefficient a is taken. Khazanov et al. first suggested values $a = 0.3$ or 0.5 but later wrote equation (4) as $2\pi r_{sh} <$ perimeter of separatrix. This perimeter comes out to be $3.23 \times r^*/\cos\alpha$, yielding a coefficient $a \approx 0.514/\cos\alpha$ in equation (4).

[10] *Khazanov et al.* [2001] took the sheath radius as [*Szuszczewicz and Takacs*, 1979]

$$r_{sh} = R + 2.5[1 - 0.616\exp(-0.32R/\lambda_D)] \times \lambda_D\sqrt{e\Delta V/kTe} \tag{5a}$$

from a fit to some numerical calculations [*Laframboise*, 1966]. Those calculations correspond to values $T_i = 0$ and $e\Delta V/kT_e < 25$, however. Here, we will use as sheath radius a

characteristic radius r_1 from asymptotic calculations at large $e\Delta V/kT_e$, giving $R^2 e\Delta V/kT_i r_1^2$ [*Sanmartín and Estes*, 1999; *Estes and Sanmartín*, 2000]; those results may be written as

$$r_{sh} = \rho_{sh} \times \lambda_D \sqrt{e\Delta V/kTe}, \tag{5b}$$

with ρ_{sh} a weak function of R/λ_D, $e\Delta V/kT_e$, and T_i/T_e. For most conditions of interest our r_{sh} is comparable though somewhat larger than values from equation (5a); for $T_i/T_e \approx 1$, $e\Delta V/kT_e \approx 10^3$ and $R/\lambda_D \approx 0.9$, we have $\rho_{sh} \approx 1.80$, making our sheath radius 1.34 times the result from equation (5a) (where the small term R is ignored). The condition in equation (4) for self-field effects is now

$$r_{sh}(\Delta V) < \frac{0.514}{\cos\alpha} r^*(I). \tag{6}$$

We note that this simple condition will grossly overestimate the effects in the extreme *cos* $\alpha \approx 0$ (or $B_0 \approx 0$) case, when it allows no electron collection whatever the current I. A tether parallel or near parallel to the geomagnetic field is of interest for no electrodynamic application, however.

[11] We finally note that equation (6) can be used in case of a thin tape too. The magnetic field created by an infinite strip of width w carrying a current I rapidly approaches azimuthal symmetry with increasing distance r from midpoint in the cross section, which is a straight segment of length w. For points collinear with that segment (upper sign below) or lying on the perpendicular at its midpoint (lower sign below), where the field is purely azimuthal, one simply has [*Bleil*, 1972]

$$B_s = \frac{I}{2\pi\varepsilon_0 c^2 r}\left[1 \pm \frac{1}{3}\left(\frac{w/2}{r}\right)^2 + \ldots\right].$$

The bracket already differs from unity by <4% at r as low as $3w/2$, or $6R_{eq}$.

3. A Self-Field Parameter

[12] The equation in condition (6) is a local relation, both ΔV and I varying along a bare tether. In the absence of self-field, universal bias-current profiles have been obtained in the past for all three modes of operation (power generation, thrust, and drag) in terms of dimesionless current and bias [*Sanmartin et al.*, 1993, 2001; *Ahedo and Sanmartín*, 2002],

$$i \equiv I/\sigma_c A_c E_m, \quad \varphi \equiv \Delta V/E_m L_* \tag{7a, b}$$

which were used by *Khazanov et al.* [2001] too. Here σ_c and A_c are conductivity and area of electrically conducting cross section, respectively, and L_* is a length characterizing ohmic effects,

$$G \times L_* \times \frac{p}{\pi} e N_\infty \sqrt{\frac{2eE_m L_*}{m_e}} \equiv \frac{3}{4}\sigma_c E_m A_c, \tag{8}$$

G being the function introduced in section 1. Also, E_m is motionally induced field along the tether, assumed vertical,

$$E_m = U_{sat} B_{0n} = U_{sat} B_0 \cos\alpha \cos\beta, \tag{9}$$

where B_{0n} is the $\overline{B}_0$ component perpendicular to the orbital plane and β is the angle between that perpendicular and the projection of $\overline{B}_0$ on the horizontal plane. The condition in equation (6) now establishes that there is no collection at tether points satisfying

$$\frac{\sqrt{\varphi}}{i} < K_s \equiv \frac{0.273 G^{1/3}}{\rho_{sh}}\left[\frac{U_{sat}}{c}\cos\beta\right]^{1/3}\left[\frac{\sigma_c/\varepsilon_0}{\Omega_0 \cos\alpha}\right]^{2/3}\left[\frac{\omega_{pl}^5 A_c^2 p}{2\pi^3 c^5}\right]^{1/3}, \tag{10}$$

where ω_{pl} is plasma frequency and we used $N_\infty = \varepsilon_0 m_e \omega_{pl}^2/e^2$ and equations (3) and (5b). Self-field effects will be greater the greater is K_s, but there are bounds to parameter values in equation (10). We recall that the condition in equation (10) will grossly overestimate those effects at small $\cos\alpha$.

[13] K_s is T_e independent and increases with density as $N_\infty^{5/6}$ if the very weak variations in both $G^{1/3}$ and ρ_{sh} are ignored; actually, $G^{1/3}$ retains values close to 1 well beyond the OML maximum radius R_{max}, and we will set $G^{1/3} = 1$ in what follows. Highest plasma densities occur in daytime for joint conditions of peak solar cycle, height around the F-layer peak, and low latitudes (save for the equatorial density trough), which we assume here. From the IRI-90 ionosphere we would typically expect a range of densities 2×10^{11} $m^{-3} - 2 \times 10^{12}$ m^{-3} from night to day. Occasional anomalously higher values, if any, would be irrelevant, slow tether operations being time-averaged.

[14] Although K_s does also increase with R, the way it does depends on the type of cross section. Cross sections other than the fully conductive circle (wire) considered by *Khazanov et al.* [2000, 2001] make for weaker B_s effects. For a wire, for a round tether conductive only on a thin outer layer of thickness h, and for a thin tape of thickness h the last bracket of equation (10) yields

$$K_s \propto R^{5/3}, \quad K_s \propto 2^{2/3} h^{2/3} R, \text{ and } K_s \propto (4/\pi) h^{2/3} R_{eq}, \tag{11a - c}$$

respectively (R_{eq} = 1/4 tape width). At equal perimeters, K_s is both smaller and a slower increasing function of R or R_{eq} in the last two cases: as regards B_s effects, tethers other than wires will be clearly less critical.

[15] There is a second reason why wires are more critical. Bias and current profiles along a tether depend on the ratio L_*/L_t ($L_t \equiv$ tether length). For both power generation and drag in deorbiting, tether operation is more efficient the lower that ratio, resulting in a short (fractional) anodic length and low collection impedance; thrust for reboost is less requiring in this respect and is considered later [*Sanmartín et al.*, 2001]. For deorbiting, efficiency, scaling with drag per unit tether mass, depends on just L_*/L_t and reaches unity at vanishing L_*/L_t if properly normalized [*Ahedo and Sanmartín*, 2002, Figure 4c]. Power generation depends on both L_*/L_t and $Z_L/(L_t/\sigma_c A_c)$, high generator-efficiency requiring a useful-load impedance Z_L that is large compared with tether resistance, though too high Z_L yields too low power, this being the usual power-efficiency trade-off of electrical generators. However, both power and efficiency increase with decreasing L_*/L_t, though, again, too small a ratio of L_*/L_t enhances ion collection and might require

insulating some cathodic segment of tether [*Sanmartín et al.*, 1993, Figures 3 and 4].

[16] The point now is that equation (8) gives

$$L_* \propto R^{2/3}, \quad L_* \propto (2h)^{2/3}, \quad \text{and} \quad L_* \propto h^{2/3} \qquad (12a-c)$$

for the respective cross sections of equations (11a)–(11c). Wires thus have L_* both comparatively large and growing with R; a thick wire may result in either too inefficient or too long of a tether. Further, and as shown in the next section, B_s effects decrease with L_*/L_t. The joint behavior in equations (11b) and (11c) and (12b) and (12c) makes such effects much less critical for tapes and round tethers conductive in a layer. In what follows we will just consider the case of wires.

[17] Since L_* varies as $E_m^{1/3}(\sigma_c R/N_\infty)^{2/3}$, L_*/L_t values at the highest plasma densities must be low enough to keep the tether operating efficiently at the lower densities. A value $L_*/L_t = 1/8$, say, at $N_\infty = 2 \times 10^{12}$ m^{-3} leads at 2×10^{11} m^{-3} to a value $L_*/L_t \approx 0.58$, still reasonably low for both power generation and drag. Taking a representative induced field $E_m = 100$ V/km and $\sigma_c = 3.5 \times 10^7/\omega$m (aluminum) we find $L_*(\text{km}) \approx 1.68 \times (R/1\text{ mm})^{2/3}$ at $N_\infty = 2 \times 10^{12}$ m^{-3}. A bound on tether length, for example 20 km, makes for an upper bound on R; setting $8L_* < L_t < 20$ km yields radius $R < 1.81$ mm.

[18] There are two points to the above. First, the very low L_*/L_t values at the high densities that are critical for self-field effects reduce any such effects. Second, a bound on radius sets a bound on K_s too, again reducing effects. To estimate K_s we rewrite equation (10) by using the centered but tilted dipole model of the geomagnetic field to relate angles α and β to modulus B_0 and orbit height and inclination i. One readily finds

$$\cos\alpha = \sqrt{\frac{4\left(B_{eq}/B_0\right)^2 - 1}{3}}, \quad \cos\beta = \sqrt{\frac{3}{4 - \left(B_0/B_{eq}\right)^2}}\,\cos(i \pm \beta_m), \qquad (13a,b)$$

and $E_m = U_{sat}B_{eq}cos(i \pm \beta_m)$; $i \pm \beta_m$ is the magnetic inclination, ranging from $i - \beta_m$ to $i + \beta_m$, $\beta_m \approx 11°$ is dipole-tilt, and $B_{eq} \approx 0.31 \times 10^{-4}$ T × (Earth radius/orbit radius)^3 is field at the magnetic equator. At 400 km height we have $B_{eq} \approx 0.26 \times 10^{-4}$ T, gyrofrequency $\Omega_{eq} \approx 0.46 \times 10^7$ s^{-1}, and $U_{sat}B_{eq} \approx 200$V/km. For the wire K_s in equation (10) takes then the form

$$K_s \approx \frac{0.236}{\rho_{sh}} \frac{\left[U_{sat}\cos(i \pm \beta_m)/c\right]^{1/3}}{\sqrt{1 - \left(B_0/2B_{eq}\right)^2}} \left[\frac{\sigma_c/\varepsilon_0}{\Omega_{eq}}\right]^{2/3} \left[\frac{\omega_{pl}R}{c}\right]^{5/3}$$

$$\approx \frac{0.388}{\rho_{sh}} \frac{\cos^{1/3}(i \pm \beta_m)}{\sqrt{1 - (B_0/0.52 \times 10^{-4}T)^2}} \left(\frac{N_\infty}{10^{12}m^{-3}}\right)^{5/6} \left(\frac{R}{1mm}\right)^{5/3}.$$

We take $cos(i \pm \beta_m) = 0.5$ (corresponding to $E_m = 100$ V/km) and a low latitude modulus, say $B_0 = 0.37 \times 10^{-4}$ T, as used in some calculations by *Khazanov et al.* [2001]. For the extreme 20 km, 1.81 mm wire setting $N_\infty = 2 \times 10^{12}$ m^{-3} and $\rho_{sh} \approx 1.8$ ($R/\lambda_D \approx 0.89$ at $T_e = 0.15$ eV) gives $K_s \approx 1.17$.

[19] In reboost, efficiency favors low L_*/L_t values in a less significant way [*Sanmartín et al.*, 2001]. Setting $L_*/L_t = 1/5$ at the upper end of the density range (making L_*/L_t barely less than unity at minimum density) takes the length $L_t = 20$ km to sensibly larger radius $R \approx 3.66$ mm and number $K_s \approx 3.20$ ($\rho_{sh} \approx 2.12$). Note, however, that tether mass would now be 2272 kg. Clearly, allowing for higher L_*/L_t values in reboost rapidly leads to greater self-field effects but also to unrealistically heavy tethers. Further, as shown in section 5, greater K_s values are actually required for self-field effects in reboost, with no effects at all for K_s below some minimum K_{smin}.

4. B_s Effects in Power Generation and Drag

[20] Bias ΔV decreases monotonically in both modes from a positive value at anodic end A (lying at the top in usual satellites moving eastward) down to a negative value at end C, where a contactor, say a hollow cathode, ejects the full electron-current collected, which flows downward (Figure 1). The rate of ΔV decrease is determined by both induced electric field and ohmic drop,

$$d\Delta V/ds = -E_m + I/\sigma_c A_c,$$

with current never exceeding the short-circuit value $\sigma_c E_m A_c$; s is distance along tether from end A. At points where electrons are collected the collection rate is given by equation (1). In terms of dimensionless variables $\xi \equiv s/L_*$, and i, φ, defined in equations (7a) and (7b), we then have

$$\frac{d\varphi}{d\xi} = -1 + i, \qquad \frac{di}{d\xi} = \frac{3}{4}\sqrt{\varphi}. \qquad (14a,b)$$

One readily finds [*Sanmartín et al.*, 1993; *Khazanov et al.*, 2001]

$$\varphi^{3/2} - i^2 + 2i = const = \varphi_A^{3/2}, \quad d\xi = -d\varphi/\sqrt{1 - \varphi_A^{3/2} + \varphi^{3/2}}.$$

[21] If the self-field is ignored, equation (14b) remains valid down to a point B where bias vanishes (Figure 1), giving

$$\varphi_B = 0, \quad \varphi_A^{3/2} = 2i_B - i_B^2, \quad \xi_B = \int_0^{\varphi_A} \frac{d\varphi}{\sqrt{1 - \varphi_A^{3/2} + \varphi^{3/2}}}. \qquad (15a-c)$$

Current is constant along segment BC (if ion collection is neglected), equation (14a) yielding $(i_B - 1)(\xi_t - \xi_B) = \varphi_C$, which reads as an equation determining the maximum current i_B,

$$(1 - i_B)\left[1 - \xi_B(i_B)\frac{L_*}{L_t}\right] = \frac{|\Delta V_C|}{E_m L_t}. \qquad (16)$$

[22] If the self-field is taken into account, however, the condition in equation (10) applies, current now remaining constant beyond a point b satisfying equations

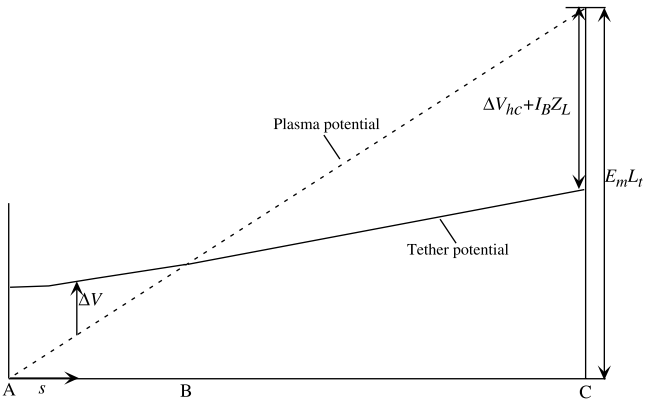

Figure 1. Voltage diagram for power generation and deorbit modes.

$$\sqrt{\varphi_b} = K_s i_b, \quad \varphi_A^{3/2} = K_s^3 i_b^3 + 2i_b - i_b^2,$$
$$\xi_b = \int_{\varphi_b}^{\varphi_A} \frac{d\varphi}{\sqrt{1-\varphi_A^{3/2}+\varphi^{3/2}}}. \qquad (17a-c)$$

Equation (14a) now yields $(i_b - 1)\,(\xi_t - \xi_b) = \varphi_C - \varphi_b$, which determines a corresponding maximum current i_b,

$$(1-i_b)\left[1-\xi_b(i_b,K_s)\frac{L*}{L_t}\right] - K_s^2 i_b^2 \frac{L*}{L_t} = \frac{|\Delta V_C|}{E_m L_t}. \qquad (18)$$

Simple estimates of current reduction can be easily obtained from equations (16) and (18).

4.1. Power Generation Mode

[23] Since the potential drop ΔV_{hc} at the hollow cathode is always very small against $E_m L_t$, the RHS of equation (16) for no self-field reads just $i_B \times Z_L/(L_t/\sigma_c A_c)$. With $Z_L/(L_t/\sigma_c A_c)$ moderately large to trade-off efficiency against power, current at end C is a moderately small fraction of the short-circuit value, with optimal i_B values around 0.15 [*Sanmartín et al.*, 1993]. Equations (15b) and (15c) yield $\xi_B \approx (2i_B)^{2/3}$ at i_B small, equation (16) becoming

$$1 \approx \frac{i_B Z_L}{L_t/\sigma_c A_c} + i_B + (2i_B)^{2/3}\frac{L*}{L_t}, \qquad (19a)$$

where the last two terms are small corrections.

[24] With self-field considered, and taking $K_s^3 i_b^2/2 \ll 1$, equation (18), using equations (17a)–(17c), becomes

$$1 \approx \frac{i_b Z_L}{L_t/\sigma_c A_c} + i_b + (2i_b)^{2/3}\left(1+\frac{1}{3}K_s^3 i_b^2\right)\frac{L*}{L_t}, \qquad (19b)$$

leading to

$$1 - \frac{i_b}{i_B} \approx \frac{4^{1/3}}{3}\left(\frac{L_t/\sigma_c A_c}{Z_L}\right)^{8/3} K_s^3 \frac{L*}{L_t}. \qquad (20)$$

Setting $Z_L = 5\,L_t/\sigma_c A_c$, say, and $L*/L_t = 1/8$ ($i_B \approx 0.157$) and $K_s \approx 1.17$ for the extreme case $L_t = 20$ km, $R = 1.81$ mm at $N_\infty = 2 \times 10^{12}$ m^{-3}, one finds $1 - i_b/i_B \approx 1.4 \times 10^{-3}$. Keeping N_∞, $L*/L_t$ (and $Z_L(L_t\,\sigma_c\,A_c)$), a tether 10 km long would have $R \approx 0.64$ mm, giving $K_s \approx 0.21$ and $1 - i_b/i_B \approx 8 \times 10^{-6}$. Note that, for any given tether, $1 - i_b/i_B \propto K_s^3 L*/L_t$ in equation (20) decreases with decreasing density as $N_\infty^{11/6}$.

4.2. Drag Mode

[25] For deboost there is no useful load. Since $\Delta V_{hc}/E_m L_t$ is very small and ξ_B reaches 4 at $i_B = 1$ in equations (15b) and (15c), equation (16) yields [*Ahedo and Sanmartín*, 2002]

$$i_B \approx 1 \quad \text{at} \quad L*/L_t > 4. \qquad (21a)$$

Considering the self-field, equation (18) gives

$$i_b \approx 1 - \frac{i_b^2}{1-\xi_b(i_b,K_s)L*/L_t}K_s^2\frac{L*}{L_t}. \qquad (21b)$$

With $\xi_b(i_b = 1, K_s)$ in equations (17a)–(17c) ranging from 4 at $K_s = 0$ to zero as $K_s \to \infty$, and $\xi_b \sim 1$ at $K_s \sim 1$, we have

$$1 - \frac{i_b}{i_B} \sim K_s^2\frac{L*}{L_t}. \qquad (22)$$

Again setting $N_\infty = 2 \times 10^{12}$ m^{-3}, $L*/L_t = 1/8$, we find $1 - i_b/i_B \approx 0.17$ and $1 - i_b/i_B \approx 5.5 \times 10^{-3}$ for the $L_t = 20$ km ($R = 1.81$ mm, $K_s \approx 1.17$) and $L_t = 10$ km ($R = 0.64$ mm, $K_s \approx 1.17$) tethers, respectively. For any given tether, $1 - i_b/i_B$ in equation (22) decreases with density as N_∞.

5. B_s Effects in Thrust

[26] In reboost, electron current flows upwards, from end A at the bottom to C at the top. Bias increases monotonically upwards at the rate

$$d\Delta V/ds = E_m + I/\sigma_c A_c,$$

with s again measured from end A. The tether is insulated over a length L_i from the top, down to a point B, to increase efficiency [*Sanmartin et al.*, 2001]. At C, where tether bias will be highly positive, a power supply gets electrons across to a hollow cathode that ejects the full collected current (Figure 2). With the collection rate still given by equation (1) where applying, we have

$$\frac{d\varphi}{d\xi} = 1 + i, \qquad \frac{di}{d\xi} = \frac{3}{4}\sqrt{\varphi}. \qquad (23a,b)$$

Since current is constant over the insulated segment BC, equation (23a) immediately gives $\varphi_C - \varphi_B = (1 + i_B)\,L_i/L*$, which reads as an equation determining i_B,

$$i_B\left[1 + i_B + \varphi_B\frac{L*}{L_t}\right] = \frac{W_e}{\sigma_c E_m^2 A_c L_i}. \qquad (24)$$

Here $W_e = I_B \Delta V_C$ is the supply electric power, with the small voltage drop ΔV_{hc} neglected.

[27] The dimensionless bias φ_B must be determined by analyzing the tether segment AB. Thruster tethers are

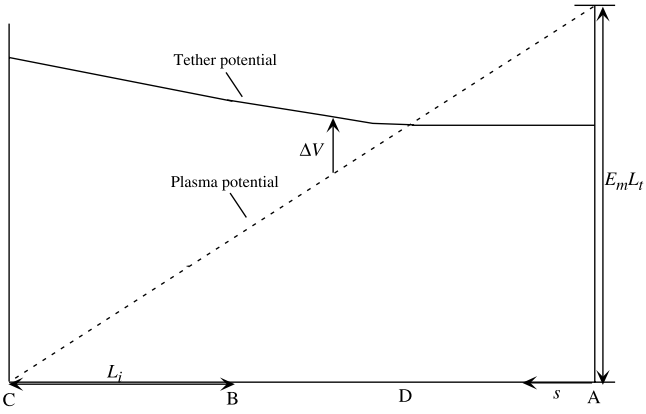

Figure 2. Voltage diagram for thrusting mode.

designed to have $\Delta V_A \approx 0$ at a nominal middensity [*Sanmartín et al.*, 2001]. At the higher densities critical for self-field effects, bias will be negative at A and vanish at some point D between A and B (Figure 2). Neglecting ion collection, current will also vanish at D. Equations (23a) and (23b) then yield

$$\varphi^{3/2} - i^2 - 2i = const = 0, \qquad d\xi = d\varphi/\sqrt{1+\varphi^{3/2}}. \quad (25a, b)$$

Ignoring the self-field, one finds at point B,

$$\varphi_B^{3/2} = 2i_B + i_B^2, \qquad \frac{L_{DB}}{L_*} = \int_0^{\varphi_B} \frac{d\varphi}{\sqrt{1+\varphi^{3/2}}} < \frac{L_t - L_i}{L_*}. \quad (26a, b)$$

Use of equation (26a) in equation (24) determines i_B, while equation (26b) is the very condition on existence of point D, occurring for low L_* (high N_∞) values.

[28] Considering now the self-field, there may be a point b above which equation (10) would apply. Use of equations (10) and (25a) would then determine $i_b(K_s)$,

$$\varphi_b^{3/2} = K_s^3 i_b^3 = 2i_b + i_b^2.$$

There exists no point b and no self-field effect, however, unless $i_b(K_s)$, which decreases with increasing K_s, is smaller than $i_B(L_*/L_i,\ W_e/\sigma_c E_m^2 A_c L_i)$, that is, unless K_s exceeds a minimum $K_{smin}(i_B) \equiv \sqrt{\varphi_B(i_B)}/i_B$; note that K_{smin} decreases with increasing i_B, reaching unity at $i_B = 2$. Design values for the ratios L_*/L_i and $W_e/\sigma_c E_m^2 A_c L_i$ at nominal density have i_B small if solar panels need be specifically dedicated to power the thruster (resulting in high power-system mass per unit power), and just $i_B < 1$ otherwise, with i_B increasing moderately in moving to the higher densities critical for self-field effects; typically, we would have $i_B \sim 0.25$ ($K_{smin} \sim 3.30$) in the first case, and $i_B \sim 1$ ($K_{smin} \sim 1.44$) in the second [*Sanmartín et al.*, 2001].

[29] Self-field effects for $K_s > K_{smin}(i_B)$ do not preclude current from growing between b and B, this being a particular feature of thrusting. If i did keep constant past b, while φ kept increasing, the ratio $K_s i/\sqrt{\varphi}$ would bounce back to values below unity, and collection as given by equation (23b) would hold; while if (23b) held, $K_s i/\sqrt{\varphi}$ would keep growing above unity, suppressing collection. Hence current will increase with φ to just keep that ratio at unity, on the threshold for B_s effects; this is a result of our approximate, simple on/off law: no collection under the condition in equation (6), full collection otherwise. At point B we would then have

$$\varphi_B' = K_s^2 i_B'^2,$$
$$\frac{L_{DB}}{L_*} = \int_0^{\varphi_b} \frac{d\varphi}{\sqrt{1+\varphi^{3/2}}} + 2K_s^2\left[i_B' - i_b - \ln\frac{1+i_B'}{1+i_b}\right] < \frac{L_t - L_i}{L_*}. \quad (27a, b)$$

[30] Replacing i_B, φ_B with values i_B', φ_B', and using equation (27a), in (24) determines i_B'. The equation

$$i_B'\left[1 + i_B' + i_B'^2 K_s^2 \frac{L_*}{L_t}\right] = i_B\left[1 + i_B + i_B^2 K_{smin}^2(i_B)\frac{L_*}{L_t}\right], K_s > K_{smin}(i_B), \quad (28)$$

relates i_B' to i_B [while $i_B' = i_B$ for $K_s < K_{smin}(i_B)$]. Assuming i_B'/i_B close to unity we find

$$\frac{i_B'}{i_B} = 1 - \frac{i_B^2(K_s^2 - K_{smin}^2)L_*/L_t}{1 + 2i_B + i_B^2(2K_s^2 + K_{smin}^2)L_*/L_t}. \quad (29)$$

In case of reboost with no dedicated solar power ($i_B \sim 1$, $K_{smin} \sim 1.44$), the 20 km, 3.66 mm, 2272 kg ($L_*/L_t = 1/5$, $K_s = 3.2$ at $N_\infty = 2 \times 10^{12}\mathrm{m}^{-3}$) wire-tether at the end of section 3 has $i_B'/i_B \approx 0.78$. That same wire would have $i_B'/i_B = 1$, however, in case of dedicated solar power ($i_B \approx 0.25$, $K_{smin} \approx 3.30$). Note that increasing K_s ($\sim R^{5/3}$) to get it well above K_{smin} rapidly increases tether mass ($\sim L_t R^2$, $L_t \sim L_* \sim R^{2/3}$) as $K_s^{8/5}$.

6. Conclusions

[31] We have considered the important point, made by *Khazanov et al.* [2000, 2001], that the magnetic field B_s created by the current of a bare tether strongly reduces its own electron-collection capability when a magnetic separatrix disconnecting ambient magnetized plasma from tether extends beyond its electric sheath. We have shown that B_s effects on collection depend on both a single dimensionless number K_s involving ambient and tether parameters and given in equation (10), and a ratio L_*/L_t parameterizing bias and current profiles along the tether ($L_t \equiv$ tether length, $L_* \equiv$ characteristic length gauging ohmic effects, defined by equation (8)); tethers operate more efficiently at lower L_*/L_t.

[32] Self-field effects are lower for lower K_s and L_*/L_t, varying as $K_s^3 \times L_*/L_t \times$ (tether resistance/load impedance)$^{8/3}$ in the power-generation mode of operation, and as $K_s^2 \times L_*/L_t$ for deorbiting. Both K_s and L_* depend critically on the type of tether cross section: We find $K_s \propto R^{5/3}$ for wires and $K_s \propto h^{2/3}R$ for thin tapes or round tethers conductive only in a thin layer, with h thickness of tape or layer (for a tape R is the equivalent radius, 1/4 *width*, of collection theory [*Sanmartín and Estes*, 2001]); length L_* varies as $R^{2/3}$ for wires and as $h^{2/3}$ for tapes and round tethers conductive in a layer. As a result, B_s-effects are fully negligible for the last two types of cross-sections, and need

only be discussed for wires, which were the tethers studied by *Khazanov et al.* [2000, 2001].

[33] With L_* increasing (while K_s decreases) with decreasing plasma density, L_*/L_t values at the highest plasma densities that are critical for self-field effects must be low enough to keep the tether operating efficiently at the lower densities; this reduces any such effects. Also, for a fixed (low) ratio L_*/L_t, wire radius, and thus K_s, decreases with wire length L_t. Self-field current reduction in deorbiting at the highest density values is < 1% for L_t = 10 km, and reaches ~15% for L_t = 20 km. Self-field effects in power generation are fully negligible in all cases.

[34] In the reboost mode there are no effects for K_s below some threshold. The threshold is lower, with significant but moderate effects in long and heavy tethers that need no dedicated solar power (low power-system mass per unit power). In a fourth mode of operation the tether floats electrically and collects ions over most of its length, acting as a source of secondary electrons for ionospheric studies [*Martínez-Sanchez and Sanmartín*, 1997]. Here B_s effects are entirely negligible because the greater mass of the collected particles (ions) results in both their greater gyroradius and lower tether current.

[35] The rapid increase of B_s effects with K_s means that strong effects will appear with parameter values taken freely in equation (10). We note that the single dramatic example of effects mentioned by *Khazanov et al.* [2001] in their abstract is in error: it corresponds to the very high density $N_\infty = 6.68 \times 10^{12}$ m^{-3} instead of $N_\infty = 1.67 \times 10^{12}$ m^{-3} (and $\alpha = 70°$ instead of 60°, with E_m = 34 V/km and R = 2.5 mm); see Figure 13 and end of section 4 in their paper. We find $K_s \approx 4.7$ for the case in their Figure 13.

[36] **Acknowledgments.** The work by J. R. Sanmartín was supported by the Comisión Nacional de Ciencia y Tecnología of Spain under grant PB97-0574-C04-1. The work by R. D. Estes was supported by NASA grant NAG8-1605.

[37] Shadia Rifai Habbal thanks Ira Katz and Manuel Martinez-Sanchez for their assistance in evaluating this paper.

References

Ahedo, E., and J. R. Sanmartín, Analysis of bare-tether systems for deorbiting low-Earth-orbit satellites, *J. Spacecraft Rockets*, *39*, 198, 2002.

Bleil, D. F., Electricity and magnetism, in *American Institute of Physics Handbook*, edited by D. E. Gray, pp. 5–26, McGraw-Hill, New York, 1972.

Estes, R. D., and J. R. Sanmartín, Cylindrical Langmuir probes beyond the orbital-motion-limited regime, *Phys. Plasmas*, *7*, 4320, 2000.

Gurevich, A. V., Distribution of captured particles in a potential well in the absence of collisions, *Soviet Phys. JETP*, *26*, 575, 1968.

Johnson, C. L., R. D. Estes, E. Lorenzini, M. Martinez-Sanchez, and J. R. Sanmartín, Propulsive small expendable deployer system experiment, *J. Spacecraft Rockets*, *39*, 173, 2000.

Khazanov, G. V., N. H. Stone, E. N. Krivorutsky, and M. W. Liemohn, Current-produced magnetic field effects on current collection, *J. Geophys. Res.*, *105*, 15,835, 2000.

Khazanov, G. V., N. H. Stone, E. N. Krivorutsky, K. V. Gamayunov, and M. W. Liemohn, Current-induced magnetic field effects on bare tether current collection, *J. Geophys. Res.*, *106*, 10,565, 2001.

Laframboise, J. G., Theory of spherical and cylindrical Langmuir probes in collisionless Maxwellian plasma at rest, *Rep. 100*, Univ. of Toronto Inst. of Aerosp. Stud., Toronto, Ont., Canada, 1966.

Laframboise, J. G., and L. W. Parker, Probe design for orbit-limited current collection, *Phys. Fluids*, *16*, 629, 1973.

Laframboise, J. G., and J. Rubinstein, Theory of a cylindrical probe in a collisionless magnetoplasma, *Phys. Fluids*, *19*, 1900, 1976.

Martínez-Sanchez, M., and J. R. Sanmartín, Artificial auroral effects from a bare conducting tether, *J. Geophys. Res.*, *102*, 27,257, 1997.

Onishi, T., M. Martínez-Sanchez, D. L. Cooke, and J. R. Sanmartín, PIC computation of electron current collection to a moving bare tether in the mesothermal condition, *pap. IEPC-01-245*, 27th International Electric Propulsion Conference, Pasadena, Calif., 15–19 October 2001.

Sanmartín, J. R., and R. D. Estes, The orbital-motion-limited regime of cylindrical Langmuir probes, *Phys. Plasmas*, *6*, 395, 1999.

Sanmartín, J. R., and R. D. Estes, Interference of parallel cylindrical Langmuir probes, *Phys. Plasmas*, *8*, 4234, 2001.

Sanmartín, J. R., E. Ahedo, and M. Martínez-Sanchez, An anodeless tether generator, in *Physics of Charged Bodies in Space Plasmas*, edited by M. Dobrowolny, p. 201, Editrice Compositori, Bolonia, Italy, 1992.

Sanmartín, J. R., M. Martínez-Sanchez, and E. Ahedo, Bare wire anodes for electrodynamic tethers, *J. Prop. Power*, *9*, 353, 1993.

Sanmartín, J. R., R. D. Estes, and E. Lorenzini, Efficiency of different types of ED-tether thrusters, in *Space Technology and Applications International Forum 2001*, edited by M. S. El-Genk, p. 479, Am. Inst. of Physics, New York, 2001.

Szuszczewicz, E. P., and P. Z. Takacs, Magnetosheath effects on cylindrical Langmuir probes, *Phys. Fluids*, *22*, 2424, 1979.

R. D. Estes, Harvard-Smithsonian Center for Astrophysics, 60 Garden Street, Cambridge, MA 02138, USA. (estes@onscreen-sci.com)

J. R. Sanmartín, Escuela Tecnica Superior de Ingenieros Aeronauticos, Universidad Politecnica de Madrid, 28040 Madrid, Spain. (jrs@faia.upm.es)